JOURNAL OF THERMOPHYSICS AND HEAT TRANSFER
Vol. 12, No. 2, April–June 1998

Combustion and Heat Transfer Interaction in a Pore-Scale Refractory Tube Burner

X. Fu,* R. Viskanta,† and J. P. Gore‡
Purdue University, West Lafayette, Indiana 47907

An axisymmetric two-dimensional model of chemical reaction and heat transfer that accounts for the transport of mass, momentum, heat, and species in radial and axial directions has been developed to provide a fundamental understanding of the transport phenomena relevant to porous radiant burners made from ported ceramics. The passage geometry of practical porous media is modeled as a cylindrical tube in which combustion takes place. This enables treatment of the chemical reactions and transport processes in the gas phase, of heat conduction in the tube wall, and of radiation exchange on the inside surface of the tube to account for the conjugate heat transfer effects. The predictions are compared with available experimental data for the purpose of model validation. Parametric calculations are performed using the model to improve understanding of the phenomena.

Nomenclature

A = pre-exponetial coefficient, $m^3/kg\ s$
c_{pf} = constant pressure-specific heat of gas, J/kg K
c_s = specific heat of solid, J/kg K
D_i = inside diameter of the tube, m
D_k = diffusion coefficient of species k in mixture, m^2/s
D_o = outside diameter of the tube, m
E = activation energy, J/kmol
F = tube-end-to-surface-element configuration factor, $F(\xi) = [(\xi^2 + 0.5)/\sqrt{(\xi^2 + x)}] - \xi$
FR = specific firing rate per unit area, W/m^2
$f_{r,\text{in}}$ = radiation fraction from the tube inlet to the surroundings
G = surface-element-to-surface-element configuration factor, $G(\xi) = \{1 - [\xi(2\xi^2 + 3)]/[2(\xi^2 + 1)^{3/2}]\}$
h = enthalpy, $(c_{pf}T_f)$, J/kg
k = thermal conductivity, W/m K
L = length of the tube, m
M = molecular weight, kg/kmol
p = pressure, N/m^2
q_r = net local radiation flux, W/m^2
R = universal gas constant, 8314 J/kmol K
Re = Reynolds number, $U_\rho D_i/\mu$
r = radial coordinate, m
S = source term in conservation equations, $1/m^3\ s$
S_{fu} = volumetric rate of fuel consumption, $kg/m^3\ s$
T = temperature, K
t = time, s
u = x-component velocity, m/s
v = r-component velocity, m/s
x = axial directional coordinate, m
Y = mass fraction
α = excess air
Γ = general transport coefficients for μ, k/c_{pg}, ρ, D_k, etc.
ΔH_c = lower heating value of methane, 5×10^7 J/kg
ε = emissivity
η = radiation efficiency, Eq. (13)
μ = dynamic viscosity, kg/m·s
ξ = dimensionless coordinate, x/D_i
ρ = density or reflectivity, kg/m^3
σ = Stefan–Boltzmann constant, 5.67×10^{-8}, $W/m^2\ K^4$
Φ = equivalence ratio
ϕ = general independent variable

Subscripts
c = centerline of the tube
eff = effective
g = gas
in = inlet
k = species
L = face at $x = L$
m = average value over cross section
o = outlet
s = solid
sur = surroundings
w = wall
0 = face at $x = 0$

Introduction

RESEARCH has recently been devoted to the mathematical modeling of submerged flame combustion phenomena within porous inert media.[1,2] In most cases a constant convective heat transfer coefficient and a one-dimensional model for flow and heat transfer have been used. Unfortunately, because of a lack of reliable thermophysical/chemical and radiative (absorption and scattering coefficients, single scattering albedo, and scattering phase function) property data of the porous matrices and interphase convective heat transfer coefficient information, many of the quantitative model predictions could not reproduce all of the available experimental data.[3–7]

Measurements of temperature and gas species concentrations within individual pores have shown important pore-scale phenomena, such as quenching of chemical reactions.[8,9] Motivated by this, a two-dimensional model accounting for transport of mass, momentum, heat, and species in axial and radial directions has been developed. The goal of the two-dimensional model is to provide a fundamental understanding of the transport phenomena relevant to porous radiant burners made from ported ceramics and metals. The geometry of a unit cell within a porous medium is modeled by a cylindrical tube in which

Received March 27, 1997; revision received Aug. 23, 1997; accepted for publication Sept. 29, 1997.

*Research Assistant, School of Mechanical Engineering, 1288 Mechanical Engineering Building; currently Senior Project Engineer, Maytag Appliances, 1801 Monmouth Boulevard, Galesburg, IL 61401.

†Goss Distinguished Professor of Engineering, School of Mechanical Engineering, 1288 Mechanical Engineering Building. Fellow AIAA.

‡Professor, School of Mechanical Engineering, 1288 Mechanical Engineering Building. Member AIAA.

combustion takes place. This enables a treatment of the chemical reactions and transport processes in the gas phase, of heat conduction in the tube wall, and of radiation interchange on the inside surface of the tube to account for the conjugate effects. In this paper, a physical/mathematical model is first described, and the model predictions are compared with available experimental data for the purpose of validation. Then, parametric calculations are performed with the model to obtain an understanding of the physicochemical phenomena.

Min and Shin[10] experimentally and analytically investigated a laminar premixed flame in a cylindrical honeycomb ceramic burner for the combustion of propane. The burner, made from cordierite, was 76 mm in diameter and 20 mm in length, and had a nominal cell density of 400 square cells per square in., i.e., the hydraulic diameter of a unit square cell was 1.1 mm, and a porosity of 0.75. Both gas and solid temperatures were measured, but the gas temperature was measured in a 26 × 1.1-mm slit formed at the center of the burner by removing the walls of 20 cells. It was reported that the range of flame stability was considerably extended by the internal heat recirculation. Two types of stable flames were observed in their experiments: a nearly one-dimensional flame, and a highly two-dimensional flame. The model developed for prediction of the thermal performance of the burner was one dimensional, in which a radiative transfer equation substantially identical to a two-flux approximation for radiative transfer in the porous medium was used. Both experiment and model predictions in the highly two-dimensional flame showed that the burning velocity and temperature of the burner flame were lower than those of the adiabatic free premixed flame. A stable flame was predicted in both downstream and upstream regions of the burner, but was not observed in the downstream region in the experiments because of heat loss from the sides. Lee and Shin[11] redesigned the burner used by Min and Shin[10] to prevent the heat loss from the sides. A stable flame was observed in the downstream region of the redesigned burner.

Before proceeding with the analysis and model development, it is appropriate to note that Churchill et al. (Ref. 12 cites some earlier references) have studied combustion and heat transfer in a refractory tube under turbulent flow conditions. To place this work in a proper historical perspective, two of the most recent references are discussed here.

Brown et al.[13] experimentally studied turbulent flow and premixed combustion of ethane in a refractory tube burner having an i.d. of 19.5 mm, an o.d. of 76 mm, and a length of 280 mm. They reported that the temperature of the gas immediately behind the flame front exceeds the adiabatic value as a result of the thermal feedback by wall-to-wall radiation and in-wall conduction. Combustion is very stable and free of oscillations because of the large thermal inertia of the refractory tube and the plug-like flow. The flame has multiple states, i.e., several discrete stable locations of the flame front, for a given flow rate and equivalence ratio. The gas temperature is nearly uniform over the cross section and is close to that of the wall as a result of the fully developed turbulent flow and strong convection between gas and solid wall. The concentration of NO_x is greatly reduced in the refractory tube compared with that in a conventional burner. Unfortunately, the range of stable flame speeds is relatively narrow.

Kansuntisukmongkol et al.[14] developed a one-dimensional model for the transient combustion of premixed propane and air inside an adiabatic refractory tube having an i.d. of 19.5 mm and a length of 254 mm. A fuel–air mixture with a fuel–air ratio of 0.0533 was used. An empirical correlation for the convective heat transfer coefficient was employed to quantify heat convection between the gas and the solid wall. Multiple steady-state solutions were predicted by the model. This is consistent with the experimental data of Brown et al.[13] Flame movement from an initial assumed location to a steady-state location was reported. The authors concluded that the wall temperature profile is the primary factor that determines the flame stability in their refractory tube.

Assumptions and Model Equations

Model Description and Equations

A straight tube (Fig. 1) is considered to represent a unit cell of a porous radiant burner with straight channels.[15] A Schwank burner is an example of the ported ceramic or metal burners under consideration here. The system could also be considered a unit cell of a ceramic foam-based burner,[9] where the complicated (tortuous) flow passage has been replaced by a straight one. Heat transfer to the gas flowing in the tube is by forced convection, and gas phase radiation is neglected because of the very small opacity of the combustion products from the very small inside tube diameter (of the order of a few millimeters). Radiation heat exchange inside the tube redistributes the heat convected from the combustion products to the inside surface. Heat conduction along the tube wall may be an important mechanism, depending upon the thermal conductivity and the wall thickness.

A schematic of the cylindrical tube unit cell considered for the treatment of the pore-level reactions, transport, and conjugate heat transfer is shown in Fig. 1. The assumptions of the model are as follows:

1) The flow channels are cylindrical and of uniform diameter along the flow direction.

2) The flow is laminar and two dimensional.

3) The outside wall of the unit cell is insulated because of the symmetry between the adjacent unit cells; conduction is the only mode of heat transfer in the inert solid phase.

4) Gas is radiatively nonparticipating because the opacity is very small based on a small tube diameter.

5) The surface of the unit cell is a gray and diffuse emitter and reflector of radiation; radiation heat exchange occurs on the inside wall of the unit cell and can be calculated using the net radiation (radiosity) method.[16]

6) Fuel, air, and products are ideal gases with negligible Dufour and Sorret effects, bulk viscosity, and dissipation.

7) Chemical reactions occur only in the gas phase, and catalytic reactions at the solid surface are negligible.

8) One-step global chemistry is used for methane oxidation.

The focus of the present study is on thermal performance of the porous radiant burners and not on the chemical kinetics or pollutant emissions. Hence, modeling of local chemical heat release is of greater interest than the determination of detailed chemistry. Furthermore, use of more detailed multistep chemical kinetics in a multidimensional (two-dimensional) computational system is beyond our computational capacity and the scope of the present study.

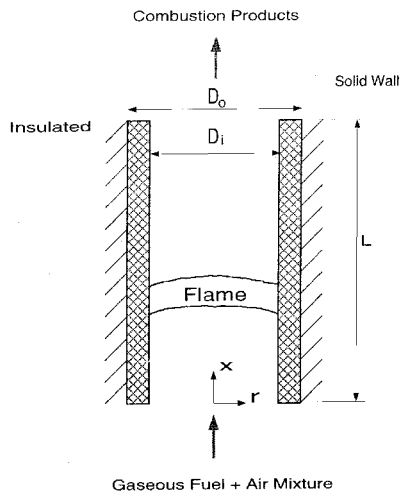

Fig. 1 Schemaic diagram of a unit cell tube with an embedded flame.

Table 1 Dependent variables in the general transport equation

Model equation	Velocity, u, v	Variable, ϕ	Transport coefficient	Source terms, Γ_ϕ
Continuity	Yes	1	None	None
x momentum	Yes	u	μ	$\frac{\partial p}{\partial x}$
r momentum	Yes	v	μ	$\frac{\partial p}{\partial r}$
Gas energy	Yes	h	$\Gamma_g = k_g/c_{pg}$	$\Delta H_c S_{fu}$
Solid energy	No	T_s	k_s/c_s	None
Species C_aH_b	Yes	Y_1	ρD_1	S_{fu}
Species O_2	Yes	Y_2	ρD_2	$(a + b/2)M_{O_2}/M_{fu}S_{fu}$
Species CO_2	Yes	Y_3	ρD_3	$-aM_{CO_2}/M_{fu}S_{fu}$
Species H_2O	Yes	Y_4	ρD_4	$-b/2M_{H_2O}/M_{fu}S_{fu}$

In view of the fact that the chemical rate constants in the global chemical mechanism have been established only for adiabatic combustion, and there is considerable uncertainty[17] in these constants, their use for nonadiabatic conditions, such as those occurring in combustion in porous media, does not appear to be warranted. The rate of fuel consumption is assumed to have the form

$$S_{fu} = A\rho^2 Y_{fu} Y_{O_2} \exp[-E/(RT_g)] \tag{1}$$

A and E are within the range of the experimental data[17] and are presented in the following operating conditions and parameters: $L = 25$ mm, $D_i = 2.9$ mm, $D_o = 3.2$ mm, $T_{g,in} = 300$ K, $FR = 315$ kW/m^2, $\Phi = 0.9$, $Re_{in} = 247$, $E = 1.3 \times 10^8$ J/mol, $A = 3.0 \times 10^8$ m^3/kg s, $k_s = 2.1$ W/m K, $c_s = 1000$ J/kg K, and $\varepsilon_s = 0.5$.

Model Equations

The assumptions in the preceding section allow the model conservation equations to be written in a general form as[18]

$$\frac{\partial}{\partial t}(\rho\phi) + \frac{\partial}{\partial x}(\rho u\phi) + \frac{1}{r}\frac{\partial}{\partial r}(\rho r v\phi) = \frac{\partial}{\partial x}\left(\Gamma_\phi \frac{\partial \phi}{\partial x}\right) + \frac{1}{r}\frac{\partial}{\partial r}\left(\Gamma_\phi r \frac{\partial \phi}{\partial r}\right) + S_\phi \tag{2}$$

where ϕ stands for u, v, T_g, T_s, and Y_k, and Γ_ϕ are the transport coefficients, and S_ϕ represents the source terms relevant to ϕ, as summarized in Table 1.

The boundary conditions at the inlet of the tube are taken to be

$$u = u_{in}, \quad v = 0, \quad Y_k = Y_{k,in}, \quad T_g = T_{g,in} \quad \text{at} \quad x = 0 \tag{3}$$

$$\varepsilon_{sur,in}\sigma(T_{sur,in}^4 - T_s^4) = -k_s \frac{\partial T_s}{\partial x} \quad \text{at} \quad x = 0 \tag{4}$$

In a combustor the gas mixture will be preheated in the inlet duct, but this is not modeled in the paper to keep the problem more generic. The effect of preheating on burner performance can be studied by changing $T_{g,in}$ and/or $T_{sur,in}$. The boundary conditions at the exit of the tube are

$$\frac{\partial u}{\partial x} = \frac{\partial v}{\partial x} = \frac{\partial T_g}{\partial x} = \frac{\partial Y_k}{\partial x} = 0 \quad \text{at} \quad x = L \tag{5}$$

$$\varepsilon_{sur,o}\sigma(T_{sur,o}^4 - T_s^4) = k_s \frac{\partial T_s}{\partial x} \quad \text{at} \quad x = L \tag{6}$$

Symmetry conditions are imposed at the axis of the tube

$$\frac{\partial u}{\partial r} = \frac{\partial T_g}{\partial r} = \frac{\partial Y_k}{\partial x} = v = 0 \quad \text{at} \quad r = 0 \tag{7}$$

On the outside surface of the tube, an insulated boundary condition is imposed as

$$-\frac{\partial T_s}{\partial r} = 0 \quad \text{at} \quad r = R_o \tag{8}$$

On the inside surface of the tube, the boundary conditions are

$$u = v = \frac{\partial Y_k}{\partial r} = 0 \quad \text{at} \quad r = R_i \tag{9}$$

$$k_s \frac{\partial T_s}{\partial r} = q_r + k_g \frac{\partial T_g}{\partial r} \quad \text{at} \quad r = R_i \tag{10}$$

The q_r in Eq. (10) on the inside wall of the tube can be expressed by an integral equation as[16]

$$q_r(\xi) - \varepsilon(\xi)\int_0^{L/D_i}\left[\frac{1}{\varepsilon(\xi')} - 1\right] q(\xi')G(|\xi - \xi'|)\,d\xi' = \varepsilon(\xi)\left[E_b(\xi) - \int_0^{L/D_i} E_b(\xi')G(|\xi - \xi'|)\,d\xi' - H_o(\xi)\right]$$

where $E_b(\xi) = \sigma T_s^4(\xi)$. In writing this equation it was assumed that the inside surface of the tube is a gray and diffuse emitter and reflector of radiation. The external radiation flux $H_o(\xi)$ incident at $d\xi$ from the two openings at the ends of the tube can be expressed as[16]

$$H_o(\xi) = \sigma T_{sur,in}^4 F(\xi) + T_{sur,o}^4(L/D_i - \xi) \tag{12}$$

Model Input Parameters

The model equations show that the thermophysical properties of the gas and the solid, the chemical reaction rate constants, the equivalence ratio (excess air), the inlet velocity (specific firing rate), and the geometry of the cell are needed as the model input parameters. The properties of the gas are calculated using the CHEMKIN program.[19]

Because the chemical reaction rate is strongly dependent on the gas temperature, the interaction of heat conduction, convection, and radiation as well as chemical heat release, which depends on the reaction constants such as A and E, play important roles in determining the flame stability. Unfortunately, accurate pre-exponential coefficient and activation energy values are not available in the published literature for reduced chemistry under nonadiabatic combustion conditions. In the present work, the activation energy for adiabatic combustion is chosen from the published literature, and the pre-exponential factor is adjusted within a range published in the literature to match the experimentally measured flame position. It is expected that all of the model input parameters may affect the

thermal performance of the system. The relative importance of these parameters is revealed through parametric calculations discussed in the following sections.

Method of Solution and Validation

The finite control volume method with a staggered grid was used to discretize the geometry and the governing equations. The discretized equations were solved using the SIMPLEC method.[18] To validate the present model, grid sensitivity studies were performed and the computational uncertainties were assessed.[20] The predicted temperatures are compared with experimental data from a parallel tube burner.

To capture the temperature gradients near the solid/gas interface, which are important in maintaining an energy balance at the interface, a nonuniform grid is used in the radial direction, and more grid points are concentrated near the interface. Grid independence studies were conducted, and a grid consisting of 75 axial nodes and 21 radial nodes, with 15 radial nodes within the gas phase, was chosen. A relative convergence criteria of 1×10^{-4} was chosen for all variables except for v, for which an absolute convergence value of 1×10^{-6} was used, because v is very small in some regions of the computational domain.

Measurements of the gas and solid temperature profiles in porous radiant burners are very sparse.[10,11,21] A comparison of the predicted solid temperature with experimental data of Min and Shin[10] is presented in Fig. 2 for propane combustion in a burner made from the honeycomb cordierite ceramic. The burner consisted of uniform duct cells with square cross sections. In the present work, the square cross section is approximated by a circular cross section so that the problem can be simplified from a three-dimensional to a two-dimensional one.

The predictions agree well with the measurements near the exit of the burner but are lower than the experimental data near the inlet (Fig. 2). The gas temperature data of Min and Shin,[10] measured in a slit of 26×1.1 mm formed at the center of the burner by removing the separating walls of 20 cells, cannot represent the gas temperature in the unit cell, because the effective cross section of the slit is much bigger than that of the unit cell. Also, the recorded gas temperatures were not corrected for the heat losses/gains. There are no appropriate temperature measurements for a pore-scale refractory tube burner available in the published literature. Therefore, a comparison of the predicted gas temperature with experimental data cannot be included in the paper.

The discrepancy between the predictions and measurements may be ascribed to the specification of the inlet and surrounding temperatures because of the fact that the structures ahead of the burner are heated, in part, by the backward radiation emitted from the burner. The measured solid temperatures indicate that preheating of the gas may have occurred by convection prior to the entrance. The predicted temperatures agree better with the experimental data if the inlet gas temperature is increased from 300 K to 500 or 800 K.[20] Inlet gas temperature between 500 and 800 K would have given the best results. The discrepancies in the predicted and measured solid wall temperature may also be related to the fact that a single-step chemical mechanism with a high activation energy is prescribed. It is possible that the low-temperature steps in the multistep realistic chemistry lead to a release of chemical energy closer to the inlet and result in higher wall temperatures.

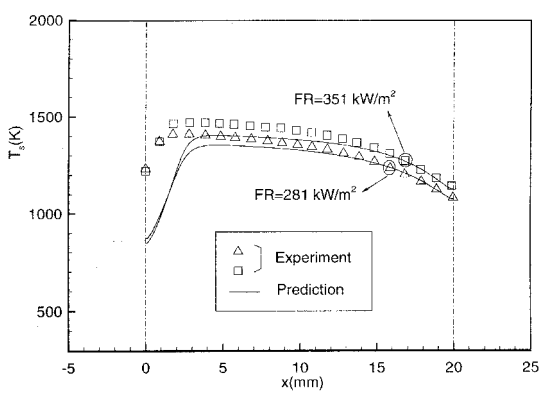

Fig. 2 Comparison of the predicted T_s with experimental data[10] for combustion of propane with $T_{gin} = 300$ K, $k_s = 2.6$ W/m K, $D_i = 1.1$ mm, $D_o = 1.27$ mm, and F = 0.55.

Results and Discussion

Baseline Simulation

Numerical simulations were carried out for a porous radiant burner made from a Celcor ceramic manufactured by Technetics Corporation.[8] The cell has a geometry with an o.d. of 3.2 mm, a thickness of 0.15 mm, and a length of 25 mm. The thermophysical/chemical properties of the burner are listed in the previous text.

To ignite methane, a chemical heat release rate (source) that is equal to the inlet firing rate was arbitrarily specified in a 1-mm-wide middle region of the tube for some time, say 4000 s, to initiate the numerical computations. The predicted transient temperatures in the tube are shown in Fig. 3. High gas and solid temperatures were generated during the ignition (preheating) time ($t < 4000$ s). After this initial time, the heat source for the ignition was terminated, and the local chemical reaction rate was computed to predict the gas temperature distribution. The flame position moved gradually upstream, and the flame finally stabilized 8 mm away from the inlet of the tube. The final flame position and steady-state performance of the burner are of primary interest; therefore, only the steady-state results are presented in the following discussion.

The coupled conduction, convection, radiation, and reaction processes can be best understood by first delineating the region in which a significant rate of reaction exists. Figure 4 shows

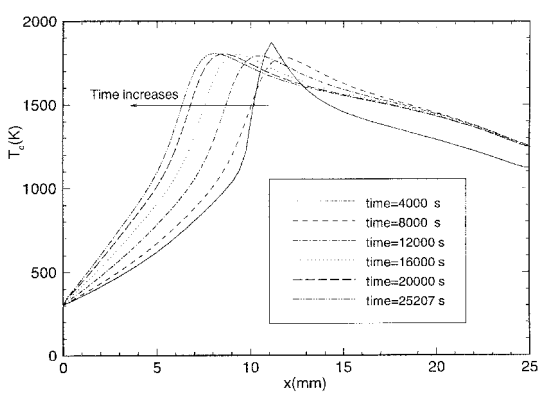

Fig. 3 Predicted transient T_c for methane combustion in a cylindrical tube.

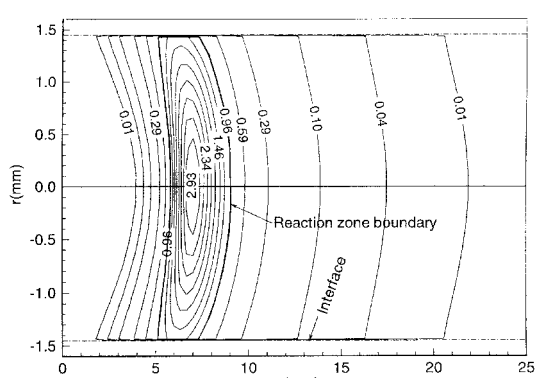

Fig. 4 Predicted reaction rate contours S_{fu} for methane combustion in a cylindrical tube.

Table 2 Maximum gas and solid temperatures, flame location, and radiation efficiency for different firing rates (flame speeds)

FR, kW/m^2	S_L, cm/s	$T_{s,max}$, K	$T_{g,max}$, K	L_f, mm	η_r, %	f_{rad}, %
236	10.2	1459	1642	8.4	38.2	18.7
315	13.7	1567	1806	8.0	36.4	17.0
415	18.0	1680	1938	8.7	35.9	12.4
515	22.3	1748	2020	11.1	36.2	6.6
550	23.8	1739	2032	14.6	37.7	2.5

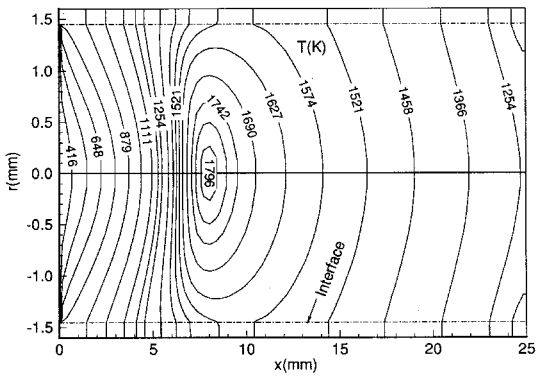

Fig. 5 Predicted T contours for methane combustion in a cylindrical tube.

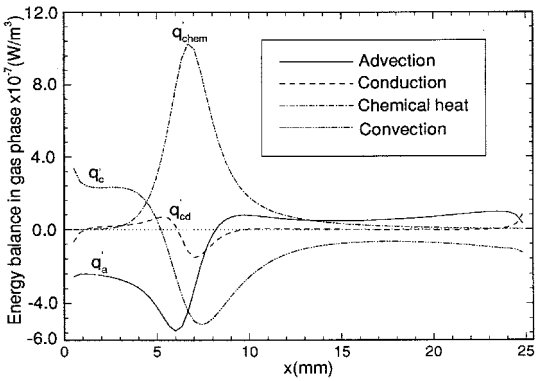

Fig. 6 Predicted q_{co}, q_{cd}, q_{ch}, and q_{chem} heat rates in the gas phase for combustion of methane in a cylindrical tube.

a contour of plots of S_{fu} within the tube. A contour representing a value of the reaction rate equal to 30% of the peak reaction rate is highlighted by a dark solid curve and labeled reaction zone boundary. The thickness of the reaction zone along the axial direction is between 3 and 4 mm. Within this zone, a major portion of the fuel is consumed. The fuel (CH_4) is not completely consumed, with 4% of the fuel leaving the burner.

Figure 5 shows a contour plot of temperature within the tube. The heat transfer processes are as follows. The gas heats the solid by convection in the reaction zone and to the right of the zone. The solid in the preheat zone is heated by conduction along the tube wall and by radiation from the high-temperature region in the reaction zone and to the right of this zone. In turn, the solid transfers heat to the gas by convection in the region to the left of the reaction zone. The tube wall and the flowing gas behave as a heat exchanger in which three heat transfer modes, i.e., convection, conduction, and radiation, occur simultaneously.

The temperature of the reaction zone does not vary significantly in the axial and radial directions. Therefore, diffusive fluxes within this region are relatively small. However, near the upstream edge of this region the temperature decreases rapidly because of gas advection, gas phase heat conduction, and species diffusion processes. The upstream heat and mass diffusion processes are strong in the axial direction. This feature is similar to that observed in one-dimensional adiabatic premixed flame propagation. The unique feature of the present configuration is that there is an equally strong diffusion of heat in the radial direction that is transferred to the solid wall. However, radial diffusion of fuel into the reaction zone is negligible compared with that in the axial direction because the solid is impermeable by the fuel.

Outside the reaction zone, the temperature profile in the gas phase is governed by a balance between the convection and diffusion processes. The gas temperature increases near the entrance of the tube because of convective heat transfer from the solid wall and lower axial velocities near the wall region, leading to large (compared to the centerline) reverse axial gas phase diffusion of heat. At approximately 5.2 mm from the entrance, the temperatures in both the gas and solid near the interface are independent of the radial distance, i.e., the temperature gradient is zero. Thus, at this location, there is no convective heat transfer between the solid and the gas. After this location, the chemical reaction in the gas phase and the diffusion of heat raise the gas temperature above that of the solid. This results in the large temperature gradient near the wall and leads to strong convective heat transfer from the gas phase to the solid wall. This process continues from the beginning of the gas phase preheat zone to the end of the tube. At axial locations between the entrance of the tube and x = 5.2 mm, there is a positive radial temperature gradient in the gas phase at the wall caused by radiative and conductive transfer from the downstream end of the solid wall to the upstream end. These mechanisms augment the preheating of the mixture in the present configuration compared to that observed in adiabatic free flames.

The flame speed is determined by the combined effects of gas preheating in the preheat zone and the heat losses by conduction and convection from the reaction zone. The maximum gas temperature, flame location, and flame speed corresponding to different firing rates are listed in Table 2. Combustion can be sustained in the tube for flame speeds ranging from 10 to 23 cm/s for the baseline parameters. The adiabatic flame speed and adiabatic flame temperature for combustion of CH_4 with ϕ = 0.9 are about 35 cm/s and 2134 K, respectively.[22] According to the theory of laminar premixed flames, the flame speed increases with an increase in unburned gas temperature and/or in flame temperature. For a given operating condition, a firing rate represents a mean flame speed that is smaller than the adiabatic flame speed. This illustrates that, although the unburned gas is preheated by convection from the solid wall, the strong radiative heat loss in the reaction zone from the inside tube surface causes a decrease in the flame temperature and a net decrease in the burning velocity. This is in contrast to nonradiant porous ceramic burners, in which superadiabatic combustion is achieved by allowing the preheat to dominate the heat transfer.[13]

The energy balance in the gas phase consists of the advective, conductive (along the axial direction), and convective heat transfer contributions, and chemical heat release. These contributions are calculated from the integral form of the energy equation, i.e., integrated over the radial direction (Fig. 6). Heat conduction in the gas is significant only in the reaction zone and near the tube entrance because of the steep temperature variation in these regions. The heat conduction rate is smaller than the heat advection and convection rates by about

Table 3 Summary of model predictions based the operating conditions and parameters of the burner

Specification	$T_{s,max}$, K	$T_{g,max}$, K	L_f, mm	η_r, %	$f_{r,in}$, %
Effect of Φ					
0.82	1539	1771	14.2	41.1	3.4
0.9	1567	1806	8.0	36.4	17.0
1.0	1562	1798	6.7	34.9	22.5
Effect of $T_{g,in}$					
300 K	1567	1806	8.0	36.4	17.0
350 K	1581	1807	7.4	36.2	19.8
500 K	1586	1809	6.3	35.6	28.2
Effect of ε_s					
0.1	1672	1882	10.4	34.5	13.1
0.5	1567	1806	8.0	36.4	17.0
1.0	1534	1783	7.7	37.5	16.6
Effect of k_s					
2.1 W/mK	1567	1806	8.0	36.4	17.0
3.0 W/mK	1550	1777	8.4	36.1	16.8
3.5 W/mK	1517	1763	8.4	36.0	17.0
Effect of $D_o - D_i$					
3.0 mm	1584	1791	7.4	36.9	18.0
3.2 mm	1567	1806	8.0	36.4	17.0
3.25 mm	1538	1781	10.0	35.5	10.5
Effect of L					
22 mm	1581	1789	8.9	38.8	12.3
25 mm	1567	1806	8.0	36.4	17.0
30 mm	1582	1817	7.2	34.4	20.9

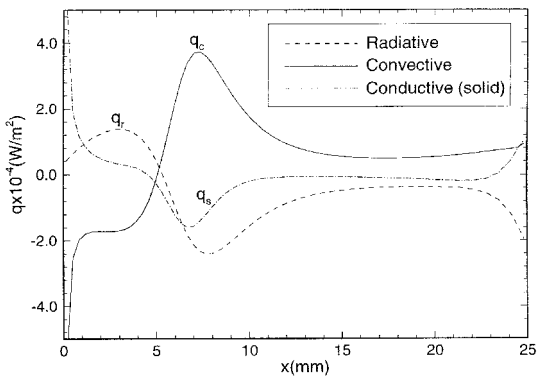

Fig. 7 Predicted q_c, q_s, and q_r normal to the interface for combustion of methane in a cylindrical tube.

one order of magnitude. This is because the gas is partly preheated by the solid. Therefore, variation of the gas temperature along the axial direction is not as large as that in adiabatic premixed combustion, in which the gas is preheated only by heat conduction.[22] This is another unique feature of the present flame in comparison with the adiabatic premixed flame. Beyond the reaction zone, the energy balance in the gas primarily consists of the convection and advection processes.

The energy balance at the interface between the solid and the gas consists of the convective (gas conductive), solid conductive along the r direction, and radiative heat flux contributions [Eq. (10)]. The local convective q_c, solid conductive q_s, and radiative q_r heat fluxes normal to the interface (heat addition to the interface is defined as positive) are plotted in Fig. 7. The net local heat flux at the wall vanishes. The solid in the preheat zone is heated by radiation from the higher temperature in the reaction zone. The radiative flux leaving the inside wall near the exit increases sharply because the surface near the exit sees the cold surroundings. Note that both the convective and conductive heat fluxes are very large near the inlet to the tube because of the steep wall temperature gradient in this region, which results from the cold gas entering the tube.

The radiation heat flux from the burner consists of two parts: 1) emission from the solid surface at the two ends, i.e., $D_i/2 < r < D_o/2$ at $x = 0$ and $x = L$, and 2) radiation from the tube inside, i.e., the interface, $r = D_i/2$. The radiation efficiency is defined as the ratio of the radiant energy leaving the end of the tube to the total chemical heat release rate of the fuel

$$\eta_r = \frac{q_r(L)\pi D_i^2/4 + 2\pi \int_{D_i/2}^{D_o/2} \varepsilon_s \sigma T_s^4 \, r \, dr}{\dot{m}\Delta H_c \pi D_i^2/4} \quad \text{at} \quad x = L \qquad (13)$$

The integral term in the numerator of Eq. (13) is the rate of radiation emission from the solid surface of the tube at the exit. For this baseline simulation, the radiation efficiency as expressed by Eq. (13) is 36%. Of this amount, 8.5% is emitted from the solid surface of the tube at the end. The fraction of total energy emitted backward from the tube, i.e., toward the inlet duct, is 17%.

Parametric Studies

The effects of the model parameters on the burner performance have been simulated. The studied parameters include *FR*, equivalence ratio, gas inlet temperature, solid emittance, thermal conductivity of solid, thickness of the tube wall, and length of the tube. A single parameter at a time is varied over a range within which the flame stabilizes in the tube. The range of some parameters is relatively narrow. This results from the limitation of the one-step chemical mechanism in modeling the stable flame range. The selected findings are summarized in Table 3 for convenience.

Figure 8 shows the dependence of the centerline gas temperature T_c along the flow direction with the firing rate. The flame location moves slightly for the low firing rates from 236 to 315 kW/m^2, but moves closer to the tube exit with the firing rate in the range from 315 to 550 kW/m^2 because of an increase in the flow rate, which requires a greater preheat area to raise the gas temperature to the combustion temperature. The unburned fuel (CH_4) mass fraction is about 4% for a firing rate of 315 kW/m^2, but is about 8% for 550 kW/m^2. This is because the flame moves closer to the tube exit as the firing rate increases. The gas temperatures within and beyond the reaction zone decrease with a decrease in the firing rate. However, the gas temperature in the entrance region decreases with the firing rate because the convective heat transfer from the solid to the gas is relatively low. Outside of the firing rate

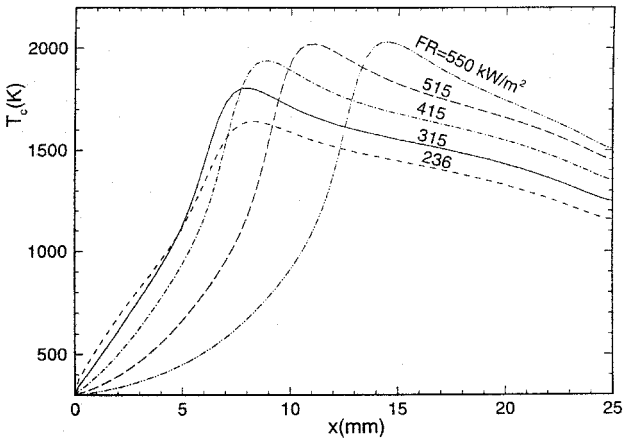

Fig. 8 Effect of FR on T_c along the tube for the baseline condition.

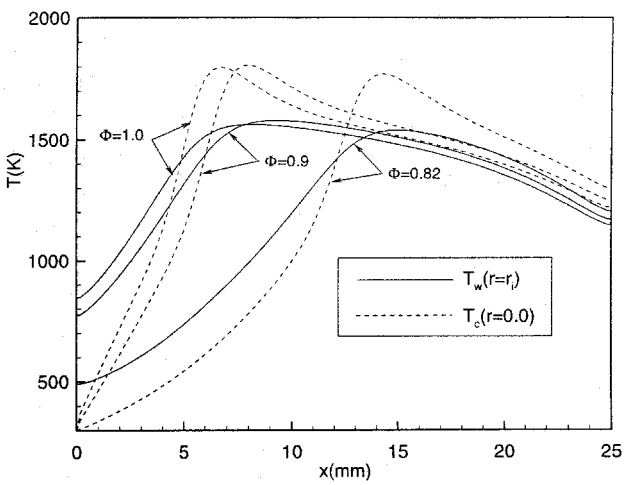

Fig. 9 Effect of F on the tube surface (solid–gas interface) and gas T_c along the tube for the baseline condition.

range from 236 to 550 kW/m^2 the flame is extinguished. The refractory tube surface temperature has been calculated,[20] and the trends with the firing rate are very similar to those of the gas centerline temperature, except that the interface temperature is about 200 K lower.

The local radiative and convective heat fluxes as a function of the specific firing rate have been computed[20] and reveal complex trends. For example, the local radiative flux increases with the firing rate within and beyond the reaction zone because of the higher solid temperatures resulting from a higher specific firing rate. However, the variation of the local radiative heat flux in the entrance region with the firing rate does not show a monotonic trend because of the complex variation of the solid temperature with the firing rate in this region.[20]

An energy balance for the entire tube as a system consists of three parts: 1) the net radiation from the tube exit to the surroundings, 2) the net radiation from the tube inlet to the surroundings, and 3) the enthalpy of the gas exiting the tube. The ratio of the first term to the rate of chemical energy release is the radiation efficiency. The ratio of the second term to the rate of chemical energy release $f_{r,\text{in}}$ decreases with the firing rate as the flame moves closer to the exit (see Table 2). The radiation efficiency decreases with the firing rate in the range from 236 to 415 kW/m^2. This is because of a relative decrease in the radiative flux from higher energy advection out of the tube at the higher firing rate. For firing rates greater than 415 kW/m^2, however, an increase in the firing rate results in a net increase in the radiation efficiency by competition between a higher fraction of energy advected out of the tube and a lower fraction of radiation from the tube inlet to the surroundings.

The effect of the equivalence ratio on the temperature distributions is shown in Fig. 9. The results reveal that the flame location moves closer to the tube exit with a decrease in the equivalence ratio. This is because a larger preheat area is needed to raise the gas temperature to the burning temperature for the gas mixture having greater excess air. From the inlet to the upstream surroundings, $f_{r,\text{in}}$ decreases with a decrease in the equivalence ratio, and the radiation efficiency increases as a result of the flame moving closer the tube exit. The flame becomes extinguished for an equivalence ratio smaller than 0.82.

The effect of the solid wall emissivity ε_s on the temperature distributions is plotted in Fig. 10. The maximum and exit gas and solid temperatures increase with a decrease in solid emissivity. This is attributed to the decrease in the radiative heat loss because of a smaller solid emissivity. With an increase in emissivity, the flame position moves closer to the tube inlet, because the preheat effect of the gas is enhanced by a higher radiation feedback from the reaction zone at a higher solid emissivity.

The effects of the solid thermal conductivity k_s and the tube wall thickness (change in the D_o of the wall) on the combustion/heat transfer inside the tube have been investigated.[20] The ranges of both k_s and the tube wall thickness for a stable flame are relatively narrow under the present operating conditions. The maximum gas and solid temperatures decrease slightly with an increase in the solid conductivity. This is attributed to the fact that an increase in the solid thermal conductivity enhances the heat conduction from the higher tem-

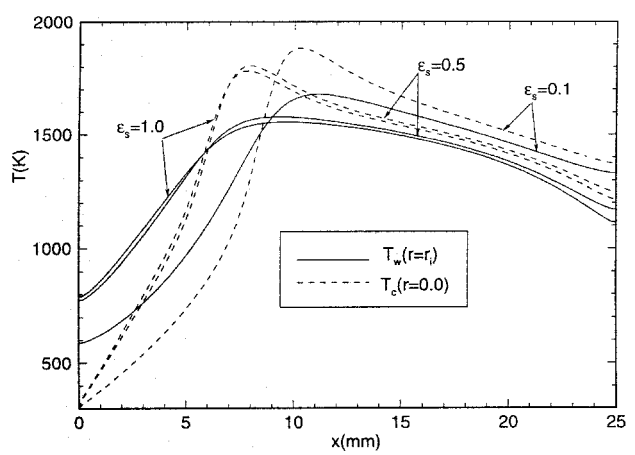

Fig. 10 Effect of «$_s$ on the tube surface (solid–gas interface) and gas T_c along the tube for the baseline condition.

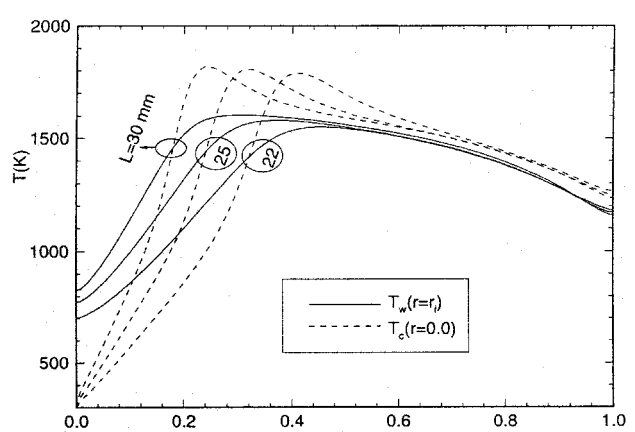

Fig. 11 Effect of L on the tube surface (solid–gas interface) and gas T_c along the tube for the baseline condition.

perature region (reaction zone) to lower temperature regions (preheat zone and zone afterreaction zone) in the solid. The flame is extinguished for a solid conductivity beyond the range from 2.1 to 3.5 W/mK under this baseline operating condition. The flame position moves away from the inlet with an increase in the outer tube diameter because the heat loss by conduction in the reaction zone increases as a result of a higher conduction area. A greater preheat area is needed to raise the gas temperature to the combustion temperature. Also, the flame is extinguished for an outer tube diameter outside the range of 3.0 to 3.25 mm under this baseline operating condition.[20]

The wall and centerline temperature variations along the tube for three tube lengths are illustrated in Fig. 11. The maximum gas temperature increases with an increase in tube length, because the radiation heat loss from the tube wall to the surroundings becomes smaller. The relative flame position L_f/L moves closer to the inlet as the tube length is increased because of a larger convective heat transfer in a longer tube. The flame is extinguished if the tube length is shorter than 22 mm.

Conclusions

Based on the results obtained, the following conclusions can be drawn for the combustion of premixed methane and air inside a small refractory tube:

1) The flame thickness in the tube is much broader than that of adiabatic combustion because of the strong conduction and radiation feedback from the high-temperature (flame) region to the preheat region.

2) There is equally strong heat diffusion in the radial direction as well as in the axial direction in the reaction zone, and, thus, the flame in the present arrangement is two dimensional.

3) Combustion occurs at a temperature below adiabatic, and flame speed is smaller than under adiabatic conditions because of the significant heat loss from the reaction zone.

4) In the gas phase, the heat conduction rate is smaller than the heat advection and heat convection rates by about one order of magnitude. This results from convection between the solid and the gas.

5) A stable flame location is determined by the strong interaction of the convection, conduction, radiation, and chemical heat release processes.

6) The peak flame temperature increases with an increase in the firing rate, a decrease in the solid emissivity, a decrease in the solid conductivity, and an increase in the tube length.

7) The radiation efficiency is calculated from the computed temperature distribution in the tube wall. Variation of the radiation efficiency with an individual parameter doesn't present a monotonic trend. This is attributed to the fact that variation in one parameter can affect convection, conduction, radiation, and chemical heat release and, therefore, temperature distribution.

Acknowledgments

This work was supported by the Gas Research Institute through a subcontract from SS Energy Environmental International, Inc. (SSEEII). J. P. Gore acknowledges partial support of this work by the National Science Foundation. The authors acknowledge numerous useful discussions with S. N. Singh of SSEEII and K. Krist of GRI.

References

[1]Howell, J., Hall, M., and Ellzey, J., "Combustion of Hydrocarbons Within Porous Inert Media," *Progress in Energy and Combustion Science*, Vol. 22, No. 2, 1996, pp. 121–145.

[2]Viskanta, R., "Interaction of Combustion and Heat Transfer in Porous Inert Media," *Proceedings of the 8th International Symposium on Transport Phenomena in Combustion*, edited by S. H. Chan, Vol. 1, Taylor and Francis, New York, 1996, pp. 84–87.

[3]Min, D., Yoo, Y., and Shi, H., "Heat Transfer in a Porous Material Having Reaction Zone," *Proceedings of the 1st KSME–JSME Thermal and Fluid Engineering Conference* (Seoul, Korea), 1988, pp. 316–322.

[4]Yoshizawa, Y., Sasaki, K., and Echigo, R., "Analytical Study of the Structure of Radiation Controlled Flame," *International Journal of Heat and Mass Transfer*, Vol. 31, No. 2, 1988, pp. 311–319.

[5]Sathe, S., Kulkarni, M., Peck, R., and Tong, T., "An Experimental Study of Combustion and Heat Transfer in Porous Radiant Burners," 1989 Western States Section/Combustion Inst., Livermore, CA, Oct. 1989.

[6]Sathe, S., Peck, R., and Tong, T., "A Numerical Analysis of Combustion and Heat Transfer in Porous Radiant Burners," *Heat Transfer Phenomena in Radiation, Combustion, and Fires*, edited by R. K. Shah, HTD Vol. 106, American Society of Mechanical Engineers, New York, 1989, pp. 146–168.

[7]Hsu, P., Evans, W., and Howell, J., "Experimental and Numerical Study of Premixed Combustion Within Nonhomogeneous Porous Ceramics," *Combustion Science and Technology*, Vol. 90, No. 1–4, 1993, pp. 149–172.

[8]Mital, R., "An Experimental and a Theoretical Investigation of Combustion and Heat Transfer Characteristics of Reticulated Ceramics Burners," Ph.D. Dissertation, Purdue Univ., West Lafayette, IN, 1996.

[9]Mital, R., Gore, J., and Viskanta, R., "A Study of the Structure of Submerged Reaction Zone in Porous Ceramic Radiant Burners," *Combustion and Flame*, Vol. 111, No. 11, 1997, 178–184.

[10]Min, D., and Shin, H., "Laminar Premixed Flame Stabilized Inside a Honeycomb Structure," *International Journal of Heat and Mass Transfer*, Vol. 34, No. 2, 1991, pp. 341–356.

[11]Lee, Y. I., and Shin, H. D., "Reconsideration on the Laminar Premixed Flames Stabilized in a Ceramic Honeycomb," *Proceedings of the 8th International Symposium on Transport Phenomena in Combustion*, edited by S. Chan, Vol. 2, Taylor and Francis, New York, 1996, pp. 1387–1397.

[12]Churchill, S. W., "Thermally Stabilized Combustion," *Chemical Engineering Technology*, Vol. 12, No. 4, 1989, pp. 249–254.

[13]Brown, M. A., Chan, C., Targett, M. J., Holtzmuller, M., and Churchill, S. W., "Combustion of Ethane with Small Concentrations of Methyl Chloride in a Refractory Tube Burner," *Combustion Science and Technology*, Vol. 115, No. 4–6, 1996, pp. 207–227.

[14]Kansuntisukmongkol, R., Miyachi, H., Ozoe, H., and Churchill, S. W., "Development of a Computational Scheme for Transient Combustion Inside a Refractory Tube," *Combustion and Flame*, Vol. 108, No. 1–2, 1997, pp. 158–172.

[15]Kilham, J. K., and Lanigan, E. P., "A Study of the Mechanism of Radiant Burners," *I.G.E. Journal*, No. 10, 1970, pp. 700–719.

[16]Modest, M., *Radiative Heat Transfer*, McGraw–Hill, New York, 1993.

[17]Westbrook, C., and Dryer, F., "Simplified Reaction Mechanisms for the Oxidation of Hydrocarbon Fuels in Flames," *Combustion Science and Technology*, Vol. 27, No. 1–2, 1981, pp. 31–43.

[18]Patankar, S., *Numerical Heat Transfer and Fluid Flow*, Hemisphere, New York, 1980.

[19]Kee, R., Miller, J., and Jefferson, T., "CHEMKIN: A General Purpose Problem-Independent, Transportable, Fortran, Chemical Kinetic Program Package," Sandia National Lab., SAND80-8003, Livermore, CA, 1980.

[20]Fu, X., "Modeling of a Submerged Flame Porous Burner/Radiant Heater, Ph.D. Dissertation, Purdue Univ., West Lafayette, IN, 1997.

[21]Hsu, P. F., "Analytical and Experimental Study of Combustion," Ph.D. Dissertation, Dept. of Mechanical Engineering, Univ. of Texas, Austin, TX, 1991.

[22]Turns, S. R., *An Introduction to Combustion: Concepts and Applications*, McGraw–Hill, New York, 1996.